Resolution evaluation of 6-degree-of-freedom precision positioning systems: Definitions and apparatus

Alain Vissiere, Sébastien Krut, Thierry Roux, Pierre Noiré, Olivier Company, François Pierrot

Resolution evaluation of 6-degree-of-freedom precision positioning systems: Definitions and apparatus

Alain Vissiere [a,b], Sebastien Krut [a], Olivier Company [a], Thierry Roux [b], Pierre Noiré [b], Francois Pierrot [a]

[a] Laboratoire Informatique de robotique et de microélectronique de Montpellier (LIRMM), Université Montpellier II / CNRS, 161 Rue Ada 34090 Montpellier, France

[b] Symetrie, 10 Allée Charles Babbage, 30035 Nîmes, France

Abstract

Resolution is a key criterion in 6 degrees of freedom (DOF) precision positioning systems such as Gough Stewart platforms. Nevertheless, there is no consensus on the definition of resolution and its evaluation. We propose a resolution characterisation method for the 6 DOF precision positioning systems based on users' requirements (in telescope and synchrotron fields). The method is founded on two user-specific criteria: stability and increment motion length. A new measurement system based on capacitive sensor technology has been developed to assess resolution. The uncertainty of our measurement system was estimated by the Monte Carlo method. This system enables measurement of hexapod platform displacement along 6 DOF with nanometre uncertainty. This is a considerable advantage because it is possible to carry out all the measures of resolution along 6 DOF automatically and without setup modification. We evaluated the resolution of an hexapod specifically developed for the Eastern Anatolia Observatory. The 6 DOF contactless measuring system enabled us to demonstrate an hexapod resolution of 20 nm for translation and 0.25 µrad for rotation.

Keywords: Resolution; precision; Nano-Positioning System; Stewart platform; Hexapod; capacitive sensor; Monte Carlo method.

1 INTRODUCTION

A positioning robot is an electromechanical system that positions objects by moving them by one or more degrees of freedom (DOF). The robot consists of a stationary platform, actuators and a mobile platform. Figure 1 illustrates one of the most conventional architectures for positioning robots, so-called Gough Stewart platforms [1] or hexapods. There are many uses for such robots: positioning samples in synchrotrons [2], microsurgery [3], metrology [4], and positioning system in telescopes [5].

The DAG (Turkish acronym for Eastern Anatolia Observatory) project is devoted to the development of a new 4m-class telescope. The telescope is composed of three mirrors: a primary mirror (M1), a convex secondary mirror (M2), and a flat mirror (M3). two hexapods enable the M2 and M3 mirrors of the DAG telescope to be into position. Figure 1 shows the CAD model of the complete telescope and the two developed hexapods. The hexapod supporting M2 is used to correct the focus, field-astigmatism and coma aberration. The hexapod supporting M3 is used to correct the focal plane tilt [6]. The developed hexapods must have a fine enough resolution to position the M2 and M3 mirrors with an better than 1 µm and 5 µrad accuracy. Resolution is thus a key criterion for the DAG project.

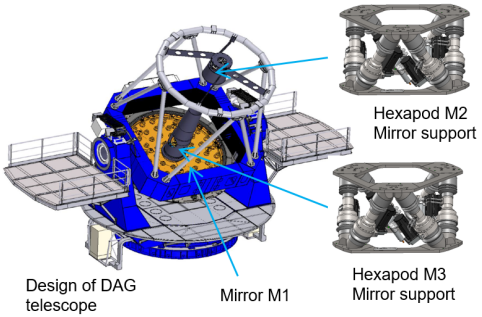

Figure 1: DAG telescope design as defined in [5] **and the CAD model of the Symetrie hexapod** [7]

The resolution concept is unclear because there is no industry standard or academic consensus. In the industry, each robot manufacturer uses its own criteria to assess resolution: Physics instruments (Pi) [8]; Newport [9]; Aerotech [10]; and Symetrie [11]. This is problematic for three reasons: it is hard to compare the performance of different robots; the proposed performance criteria are not always tailored to users' needs and the evaluation methods are often not specified.

Few scientific studies deal with the positioning system resolution issue. Furthermore, these studies concern only nano-positioning systems with only one or two DOF. As specified in [12], the strokes considered are very short, i.e. in the 100 µm range. The resolutions achieved are subnanometric. In several studies [12] [13] [14], the resolution is defined as the sensor resolution limit used for closed loop position control. In this case, Flemings specifies in [12] that external disturbances are neglected. However external disturbances markedly reduce the resolution level.

The present paper is focused on the study of 6 DOF positioning robots with at least 100 mm strokes. In the first part, we propose a new resolution characterisation method based on users' needs (in the telescope and synchrotron fields). Then a setup to measure the resolution in 6 DOF with nanometer accuracy is presented. The uncertainty of the new measurement system was estimated by the Monte Carlo method. An example of resolution measurement (20 nm and 0.25 µrad) is illustrated in the last part of this paper.

2 RESOLUTION DEFINITION FOR POSITIONING ROBOTS

There is no standardized definition for the resolution concept regarding positioning systems. For this reason, manufacturers have put forward their own definitions. Thus, Symetrie [16], [17] PI, Aerotech [18] or Newport [19] propose to distinguish the theoretical resolution and the resolution or minimum incremental motion (MIM). Table 1 presents terminologies and definitions that are used by all of the manufacturers (Newport, PI, Aerotech, Symetrie).

Vocabulary used		Theoretical resolution, display resolution, Resolution, practical resolution, minimum, encoder resolution, design resolution, incremental motion (MIM), typical resolution
Manufacturers definition	Newport [8]	"Resolution, also referred to as display or encoder resolution, is the smallest increment that a motion system can be commanded to move and/or detect." "Minimum incremental motion (MIM) is the smallest increment of motion a device is capable of **consistently** and **reliably** delivering."

niti ons		
Pi [9]	"Design resolution: The theoretical minimum movement that can be made."	"The smallest motion that can be **repeatedly** executed is called minimum incremental motion, or typical resolution, and is **determined by measurements**."
Aerotech [10]	"Theoretical resolution may exceed practical resolution"	"Practical resolution: The smallest possible movement of a system."
Symetrie [11]	"Theoretical resolution"	"The resolution or minimum incremental motion (M.I.M.) is the smallest increment that the machine can perform."

Table 1: Manufacturers' definitions (Newport, PI, Aerotech, Symetrie)

According to the International Vocabulary of Metrology (VIM) [12], resolution is defined as the "smallest change in a quantity being measured that causes a perceptible change in the corresponding indication". Based on this definition we can give a qualitative definition for positioning system resolution: ***Resolution*** – also called the minimum incremental motion (MIM) – is the smallest increment of motion that a robot is capable of performing.

Theoretical resolution – also called display resolution, encoder resolution or design resolution – is the shortest distance that can theoretically be travelled. The theoretical resolution is generally calculated from the resolution of the encoder engine. A multiplying factor is used for all movement converting system between the encoder engine and the hexapod platform displacement.

2.1 Criteria and method to evaluate resolution

Movement increment must be more precisely defined to evaluate MIM.

2.1.1 Position stability

Stability is the capacity of a positioning system to keep the same position over time. It is a fundamental characteristic of a positioning system. The stability assessment conditions should be precisely defined: time scale, measurement direction (translation, rotation), fixed and variable loads, vibrational excitation (shocks, machines nearby) and temperature (controlled or not). To distinguish two successive motion increments, the movement increment value must be greater than the platform position instability level.

First criterion

Relative stability: the amplitude variations of the position – between two motion increments – must be less than 10% (empirical value) of the movement increment value.

The 10% value has to be tailored to the users' needs in the project.

2.1.2 Motion increment length

The motion increment length has to be consistent with the commanded length to ensure that the systemis in the right position. For these reasons we propose the following second criterion

Second criterion

Motion increment length: **commanded increment length -30% < increment length < commanded increment length +30%**

The 30% value has to be tailored to the users' needs in the project. These two criteria –

stability and motion increment length – allow us to quantify the hexapod resolution.

2.1.3 Example of resolution test results

Figure 2 shows an example of a resolution test. The hexapod platform was translated along the Y axis by 10 successive 100 nm steps. The top graph on Figure 2 shows the platform position along the Y axis. The dotted red line represents the tolerance stability limit. The bottom graph on the Figure 2 shows the amplitude of the 10 steps. The red line shows the the step length tolerance limit. Each step value has to fall between 70 nm and 130 nm to satisfy the length criteria. In the case of Figure 2, the stability criterion and motion increment length criterion were met.

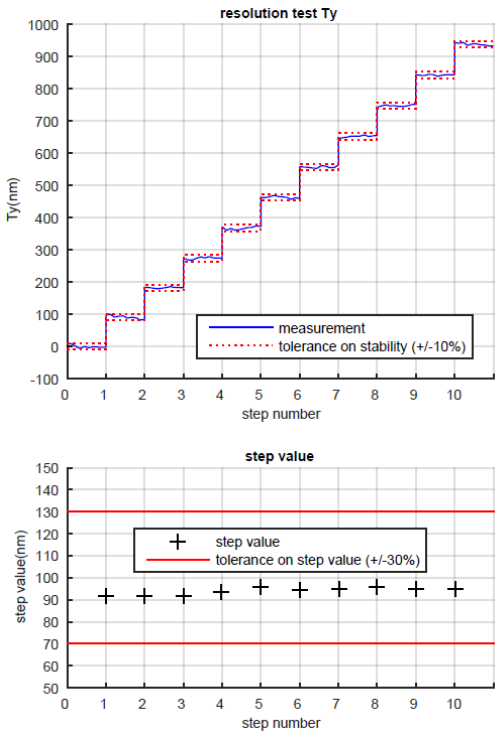

Figure 2: Example of a resolution test.

Two preliminary treatments were conducted on the raw data before plotting the curves in Figure 2. Firstly, data recorded during displacements was systematically removed. The platform position during motion increment is not related to the resolution concept. Secondly, real-time filtering was applied to the raw data. This filtering is described in paragraph 3.2. Then 10 points were recorded between two motion increments at a 1 Hz acquisition frequency.

In the case in Figure 2, motion is along one axis and one direction. For many applications, the hexapod is used along 6 DOF with direction inversion, e.g. to adjust the telescope mirror

position by translation and rotation. Therefore, tests are commonly carried out with direction inversion. Figure 3 presents the results of such a test for the Y axis. The bidirectional resolution test presented is an extension of the pure resolution concept. As in the Figure 2 case, the stability criterion and motion increment length criterion were fulfilled.

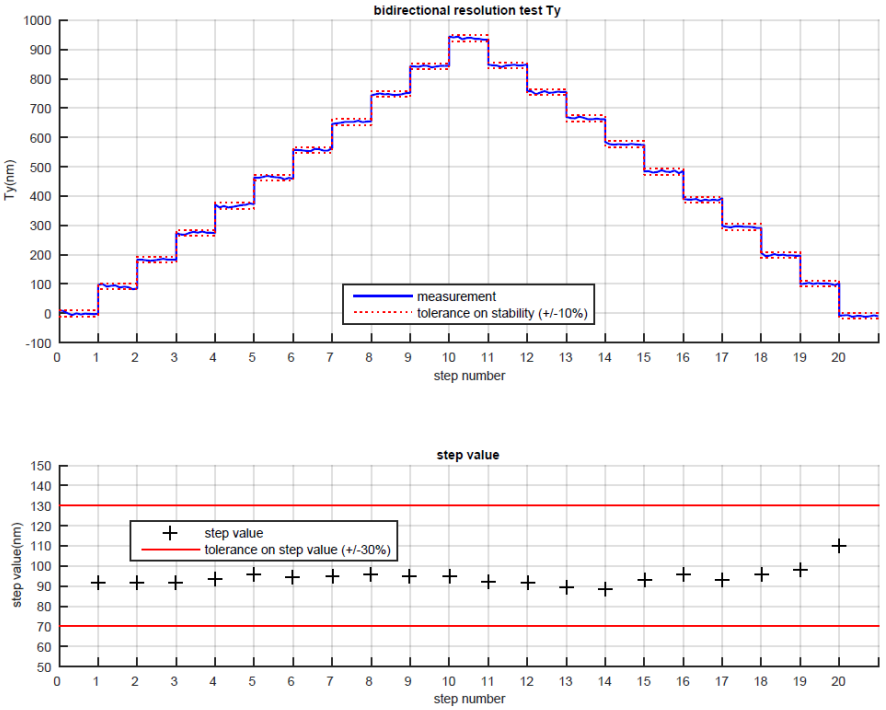

Figure 3: Example of a bidirectional resolution test. Y axis and 100 nm step

3 RESOLUTION MEASUREMENT

A setup dedicated to resolution measurement have been developed. This system is based on the use of capacitive sensors. It allows to perform displacements measurements according to 6 DOF. This is a considerable advantage because it is possible to carry out all resolution measurements along 6 DOF automatically and without any setup modification.

3.1 ARCHITECTURE OF THE 6 DOF SETUP

The measurement system principle is described in Figure 4. Six displacement sensors are attached to the base of the hexapod via the (green) support. These 6 sensors measure the motion of a target attached to the moving platform according to 6 DOF.

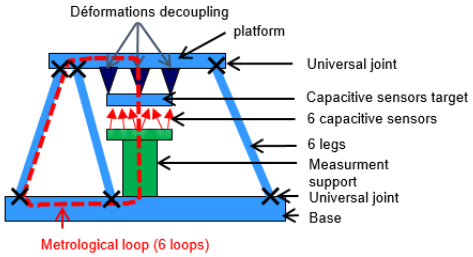

Figure 4: Measurement system

Metrologists use the of metrology loop concept to evaluate and optimize the design of measurement machines [13][14][15]. The metrology loop is defined as a conceptual line going through all solids, sensors and joints of a machine and determining the relative position of probes with respect to the artefact. The artefact is the part to measure – it could for instance be a simple cylinder [14]. Any non-controlled dimensional change in the metrological loop increases the measurement uncertainty. Hence, the dimensional stability of all components crossed by the metrology loop have to be optimized.

The metrology loop concept can be tailored to our resolution measurement system. The artefact is the hexapod in Figure 4. The dimensional stability of components crossed by the metrology loop (red in Figure 4) has been optimized. We designed the most compact and stiff metrological structure to minimize the deformation amplitude. We used INVAR to reduce the temperature variation impact because of its low thermal expansion coefficient (0.15 µm/m/ °C). In addition, the setup was placed in a measurement room with small temperature variations (0.05°C). The hexapod platform was deformed under the strain induced by the six actuators. We developed a specific decoupling system to avoid transmitting deformations from the platform to the capacitive sensor target. The target is connected to the platform through 3 decoupling blades facing 120° (triangles in Figure 4). The principle and implementation of this decoupling liaison is explained in [20]. The detailed design of the decoupling system and the capacitive sensor target is presented in Figure 6.

We opted to evaluate the hexapod resolution in the same conditions as will be used to position the DAG telescope M2 mirror. Consequently, the hexapod was returned and a mass was added under the platform to simulate the weight of the telescope mirror. The configuration is presented in Figure 5.

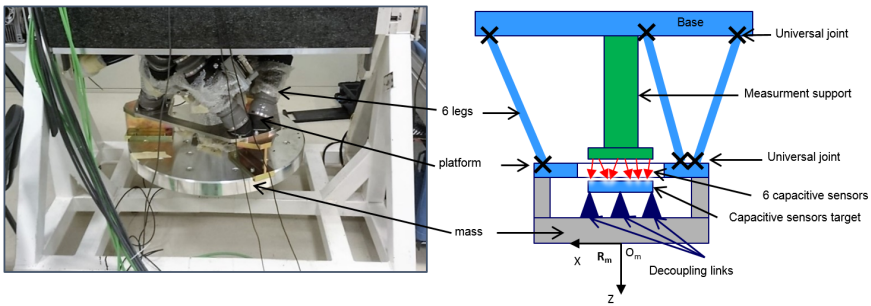

Figure 5: Hexapod configuration for the resolution test

To define the pose of the hexapod, we introduced the base frame (denoted R_b) and the mirror frame (denoted R_m). R_m is attached to the mass as shown in Figure 7. R_b is attached to the hexapod base. For the ease of experiments R_b was chosen coincident with R_m for the initial pose of the resolution tests.

The pose is described by the pose vector χ.

Where T_x, T_y and T_z are the translations and R_x, R_y and R_z are the rotations of the mirror along the fixed axis of the base frame R_b.

3.2 Sensor choice and data acquisition

Sensors have to provide high accuracy and resolution for our 6 DOF measuring system. Typically, to measure an MIM of 10 nm – according to the resolution criteria presented in this paper – the sensor has to provide a measurement error of less than 1 nm and a resolution better than 1 nm. Interferometric or capacitive sensors are the most commonly used to achieve this performance level [16]. In [17], the capacitive sensor residual error after calibration was experimentally reduced to less than 1 nm in an 80 µm range. Capacitive sensors are less expensive than interferometers and they have a smaller footprint. We thus chose capacitive sensors for our 6 DOF measuring system.

The use of commercial capacitive sensors has to be optimized to achieve measurements with sub-nanometer uncertainty. Two categories of error, as described in [16], should be minimized: systematic and random error. An interferometer based calibration is required to reduce the systematic error. The interferometer is considered as the reference measurement. The reference interferometer is traceable to the International System of Units (SI). The residual error is less than 0.1% of the travel range after calibration.

The capacitive sensor random error is caused by electrical noise. All electronic components produce small random changes in voltage potential that combine throughout the circuitry and appear as a band of noise [18]. The recorded data reveals that the capacitive probe noise is about 40 nm and has a Gaussian distribution. This implies that the measurement can be improved by applying a filter. For our tests, a Butterworth low pass filter was applied to the measurement values. For all the tests, we empirically chose a 1 Hz cutoff frequency.

The graph in Figure 6 presents the complete architecture of the acquisition system. The six capacitive sensors are connected to the conditioner module [19]. An analog-to-digital converter is used to generate digital values from the conditioner module output. A software package applies the Butterworth low pass filter. The tests are automated and conducted remotely to minimize environmental disturbance (thermal, vibration). Consequently, a trigger signal is sent by the PC to automatically control the motion of the hexapod following a duty cycle.

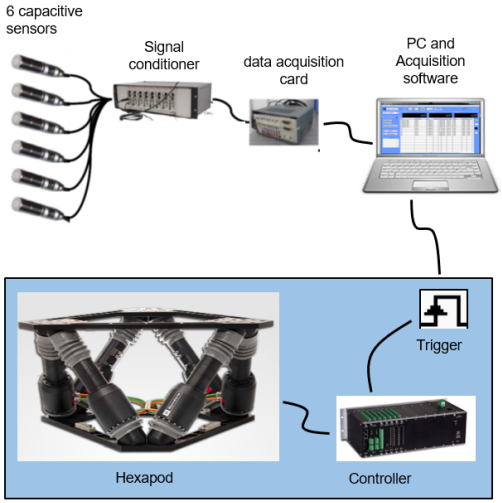

Figure 6: Data acquisition architecture

3.3 From capacitive sensor values to platform position

Figure 7 shows the detailed design of the capacitive sensor target. The surfaces targeted by capacitive sensors are the areas shown in green. We recall here that Tx, Ty and Tz denote the translations and Rx, Ry and Rz denote the rotations of the robot platform along the fixed axis of the base frame denoted Rb (see paragraph 3.1 figure 5). For Tz translation and Rx and Ry rotation, three capacitive sensors oriented along the Z axis measure the translation of three discs located on the XY plane. For Tx translation and Rz rotation two capacitive sensors are oriented along the X axis and target the central block. For Ty translation, a sensor oriented along the Y axis targets the central block.

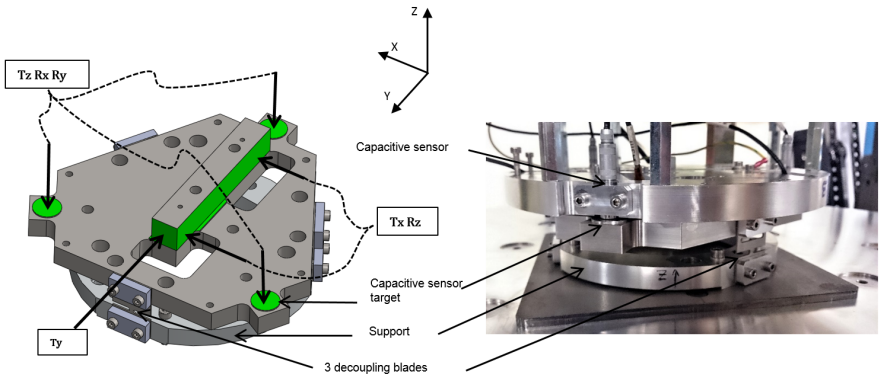

Figure 7: Detailed design of the measurement system

At that point, the mirror frame displacement has to be deduced from the 6 capacitive sensor measurements through the forward kinematics of our measurement system. Figure 8 shows the complete settings of the measurement system: capacitive sensor targets and capacitive sensor support.

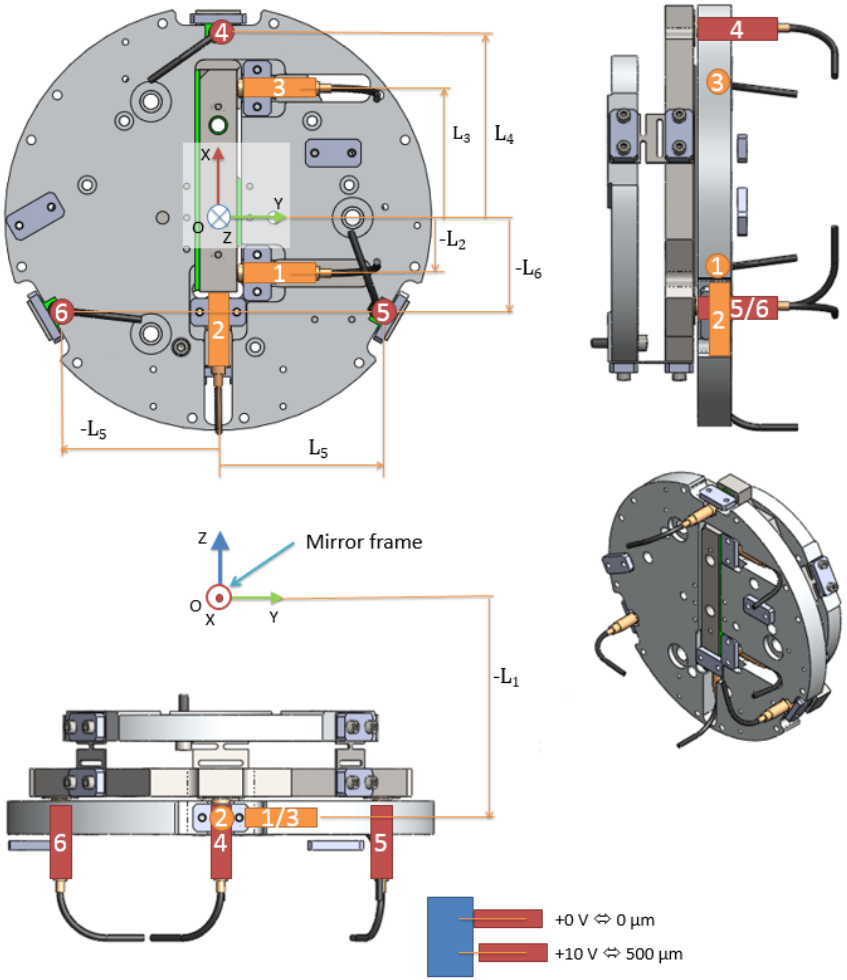

Figure 8: 6 DOF measurement system

length	Value (m)
L_1	0.4020
L_2	0.0300
L_3	0.0700
	0.1000
L_4	0.0866
L_5	0.0500
L_6	

Table 2: Capacitive sensor positions

The value given by capacitive sensors is denoted C, where

The first step consists of expressing the value given by each capacitive sensor depending on χ components. For the first capacitive sensor, denoted C_1:

Similar equations for the 6 capacitive sensors give the following relation:

By inversing M in equation (5):

By equation (6), the displacement of the mirror frame is deduced from the 6 capacitive sensor measurements.

4 UNCERTAINTY ESTIMATION BASED ON THE MONTE CARLO METHOD

To estimate measurement uncertainty, two methods are detailed in the "Guide to the expression of uncertainty in measurement" (GUM)[20][21]. The first method proposed in the GUM is based on the law of propagation of uncertainty. The application of this first method becomes tedious, especially when the measurement process is complex [22]. The Monte Carlo method (MCM) offers an alternative to estimate uncertainty.

We chose the Monte Carlo method in order to estimate the measurement uncertainty of our 6 DOF measurement system. In the present study, the different MCM steps described in the GUM were applied:

- definition of the measured output quantity
- definition of the input quantities upon which the output depends
- determination of the probability density function (PDF) of the input variables
- definition of a model relating input and output
- Propagation of PDFs for input through the model to obtain the PDF for output
- estimation of the standard deviation and confidence interval for output.

Our resolution evaluation proposal is based on two criteria: stability and motion increment length. Firstly, we implemented the Monte Carlo method to estimate the stability measurement uncertainty. In this case, the measurand is the position of the platform for 10 s. The input variables are the 6 values given by the 6 capacitive sensors. To estimate the PDFs of the 6 input variables, 90,000 values per capacitive sensor were recorded for a test duration of 100 s. For this data capture, the position of the target sensor was assumed to be perfectly stable. The result of the test is presented in Figure 9. The histograms show the recorded sensor values. A normal probability distribution function – represented by the red dotted line – was fitted to the recorded data. The mean value, denoted μ, was removed for clarity. The

standard deviation, denoted σ, ranged from 1.35 to 1.74 nm.

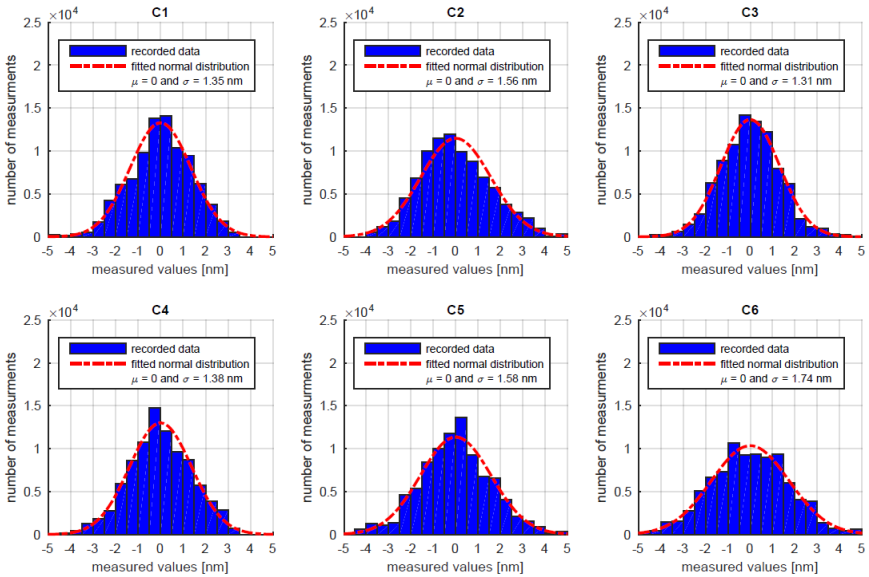

Figure 9: Normal distribution for the six capacitive sensors

The forward kinematics of our measurement system were used for PDF propagation. Two cases were studied here. In the first case, platform displacement was calculated in the capacitive sensor plane (in Figure 8, distance L1 is equal to zero). In the second case, displacement was calculated at 40.2 cm above the capacitive sensor plane (in Figure 8, distance L1 is equal to 40.2 cm).

The Figure 10 histograms show the calculated positions. Actually 100,000 values were randomly generated according to the six normal distributions experimentally identified for the six capacitive sensors. Then the generated values were input into equation (6) to calculate 100,000 platform positions along each of the 6 DOF. In Figure 10, normal probability distribution functions – represented by dotted lines – were fitted to the calculated platform positions. The red dotted line refers to L1=0 and black dotted line refers to L1=40.2 cm.

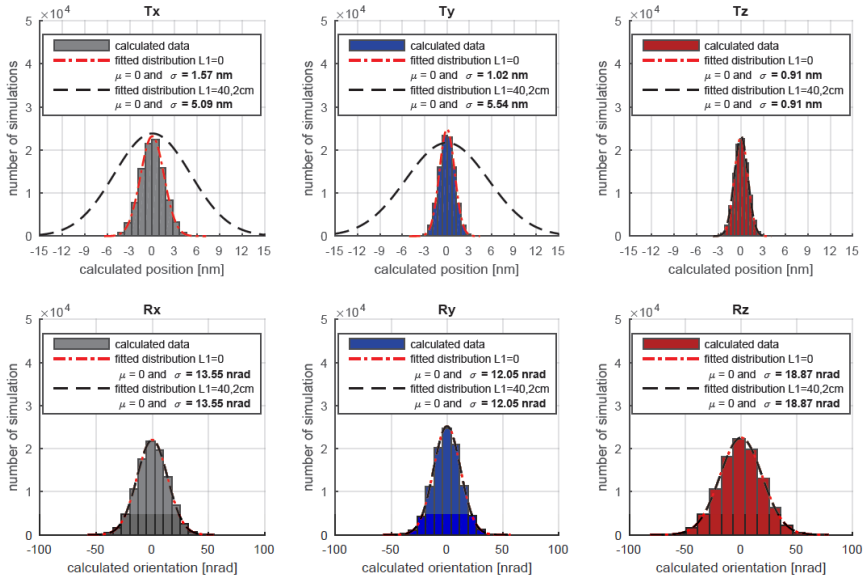

Figure 10: Platform position simulations along the 6 DOF

The standard deviation obtained with L1=0 ranged from 0.91 to 1.57 nm for the platform position measurements and from 0.012 to 0.019 µrad for the platform orientation measurements. The position measurement uncertainty was slightly better than the individual capacitive sensor uncertainty due to the averaging effect. For example, displacement along the Z axis is the mean of sensors 4 to 6.

Figure 10 highlights the effect of the L1 distance on the stability measurement uncertainty. Indeed, when L1 increased from 0 to 40.2 cm, the standard deviation increased by approximately 4 nm for the X and Y axes. Tz translation and Rx, Ry and Rz rotation were not affected by the L1 distance. The best solution – to avoid the uncertainty amplification – was to design a tailored sensor support to minimize the L1 distance. The uncertainty, and the 95% coverage interval for the stability measurement, are listed in Table 3 for L1 = 0.

Table 3: Uncertainty of the 6 DOF measurement system

Axis	Uncertainty	95% coverage interval
Tx(nm)	1.56	[-3.12 , 3.12]
Ty(nm)	1.02	[-2.04 , 2.04]
Tz(nm)	0.91	[-1.82 , 1.82]
Rx(µrad)	0.014	[-0.028, 0.028]
Ry(µrad)	0.012	[-0.024, 0.024]
Rz(µrad)	0.019	[-0.038, 0.038]

Secondly, the uncertainty on the step length measurements was studied. Here the only source of uncertainty was related to the trueness of the capacitive sensors. After calibration, the residual linearity error of the 6 capacitive sensors was less than 0.1% of the measurement range. The effect of this error on the step length measurements was less than 0.7% on the translation and less than 0.3% for the rotations. As 30% is the usual value for the step length

criterion, we considered that the systematic error introduced by our measurement system was negligible.

5 EXPERIMENTAL RESULTS AND DISCUSSION

The resolution test was conducted to evaluate the resolution of the DAG project hexapod. The hexapod resolution was not known before the test. Consequently, we tried different resolutions from the high to low to empirically determine the achievable resolution level. The test cycle is described on the following table.

Table 4: Test cycle

	Translation Tx	Translation Ty	Translation Tz	Rotation Rx	Rotation Ry	Rotation Rz
number of roundtrips	step size (nm)	step size (nm)	step size (nm)	step size (µrad)	step size (µrad)	step size (µrad)
1	500	500	50	0,5	0,5	0,5
3	200	200	20	0,25	0,25	0,25
3	100	100	10	0,1	0,1	0,1

Figure 11 gives an overview of the test results. The 6 DOF were tested successively. The graph position was initialised at zero.

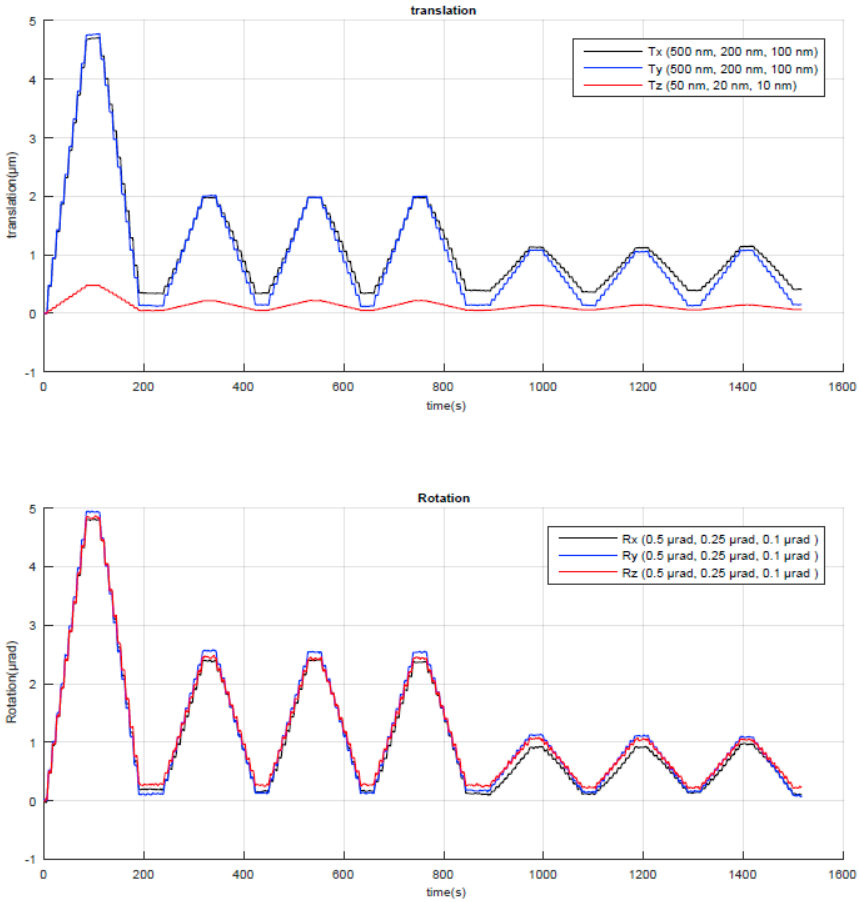

Figure 11: Overview of the complete test results (Tx Ty Tz) and (Rx Ry Rz)

Figure 12 shows zoomed views of 6 achieved DOF resolutions.

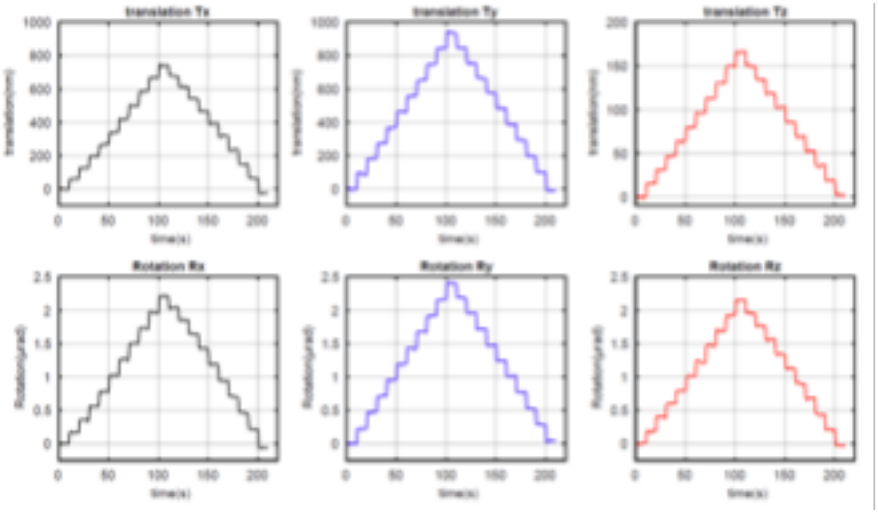

Figure 12: Zoom resolutions Tx, Ty, Tz and Rx, Ry, Rz

The tested hexapod achieved a resolution of 100 nm along the X and Y axes and 20 nm along Z. This difference could be explained by a simple stiffness analysis. According to [23], stiffness along the Z axis is higher than that along the X or Y axes. This inequality is always true if the hexapod height is greater than the difference between the base and the platform radius. This condition was verified for the studied hexapod. Stiffness along the Z axis was greater than that along X or Y axes. Consequently, the stability in relation to vibrations was better along the Z axis.

The step length along the Y axis was 100 nm and consistent with the specification. The steps were smaller than the command for the X and Z axes. The first hypothesis was that the difference between the command and the effective step length was due to the accuracy of the hexapod along the total travel range. However, the accuracy had already been evaluated using a coordinate measuring machine (CMM): after hexapod calibration [24][25] the motion error was less than 10 µm for a 10 mm travel range and along the 3 DOF. By extrapolating this result to a smaller range, the accuracy error turned out to be better than 1 nm for a 1 µm length step, which could be neglected. The second hypothesis was that the accuracy difference between the 3 axes could be due to the joint configuration difference. To confirm this hypothesis, it was necessary to investigate the hexapod behaviour, which did not concern the method and resolution measuring system.

The platform orientation was evaluated by calculating the difference between two or three capacitive sensor values. In this case, the capacitive sensor target was tilted relative to the sensor axis. It is questionable whether it was necessary to take the effect of tilt on the capacitive measurement into account. Firstly, the target tilt was the same for all of the capacitive sensors. Consequently, the tilt effect would be cancelled out when calculating the sensor measurement difference. Secondly, experiments described in [18][26] showed that the capacitive sensor tilt had a negligible effect – at the nanometer scale – for lower slopes than +/- 87 µrad. The maximum tilt for our test was under 5 µrad.

The tested hexapod achieved 0.25 µrad resolution along X, Y and Z axes. The rotation amplitude was less than the command for the X and Z axes. This point will need to be investigated further. However, as for translation, that aspect concerns the hexapod more than the resolution measurement method and device.

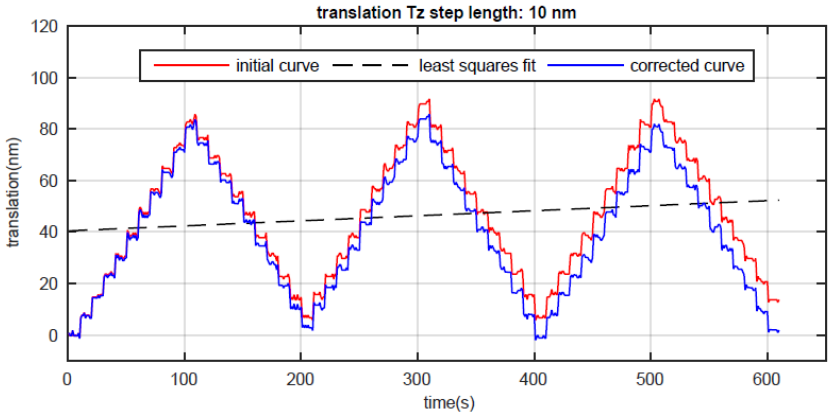

Figure 13: Thermal drift compensation

Figure 12 shows an example of resolution measurements for three cycles. There was an offset of 14 nm between the first and last positions. This offset could be explained by thermal drift of the system over the duration of the test (10 min). Thermal drift was not related to the resolution evaluation. Consequently, it would be of interest to try to remove the thermal drift effect by post processing. In Figure 13, the thermal drift effect was considered to be linear. The least-squared best-fit line (dotted line) was deleted from the intial results (red line). The blue line is the resolution test result after deleting the thermal drift effect. This method must be conducted with care. Indeed, the thermal drift estimation could be distorted by mecahnical hysteresis phenomena, so it should be carried out over at least two duty cycles.

5.1 Conclusion

The present study focused on the resolution evaluation of 6 DOF positioning robots. A new resolution characterisation method has been proposed. The method is founded on two criteria based on the users' needs: stability and motion increment length. A new setup to measure the resolution in 6 DOF was developed to achieve characterisation at a nanometer level. The uncertainty of the measurement system was estimated by the Monte Carlo method. The uncertainty achieved was better than **1.5 nm for the positions and 0.02 µrad for the orientations.** The capacitive technology based device was tested on an hexapod and the following resolution was obtained: Tx,Ty: 100 nm, Tz: 20 nm Rx,Ry,Rz: 0.25 µrad.

Acknowledgments

The authors would like to acknowledge the financial support obtained from the French National Research Agency (Project ANR-15-LCV3-0005). We are also grateful to Mathieu Cuq, Engineer at Symetrie, for his help.

5.2 References

[1] D. Stewart, A platform with six degrees of freedom, ARCHIVE: Proceedings of the Institution of Mechanical Engineers 1847-1982 (Vols 1-196). 180 (1965) 371–386. doi:10.1243/PIME_PROC_1965_180_029_02.

[2] Q. Lu, Y. Li, Z. Peng, Nuclear Instruments and Methods in Physics Research A Kinematics analysis of

six-bar parallel mechanism and its applications in synchrotron radiation beamline, Nuclear Inst. and Methods in Physics Research, A. 674 (2012) 8–14. doi:10.1016/j.nima.2012.01.003.

[3] H.F.F. Mhsc, W. Wei, R.E. Goldman, N. Simaan, Robot-assisted ophthalmic surgery, Canadian Journal of Ophthalmology. 45 (2010) 581–584. doi:10.3129/i10-106.

[4] A. Mura, Mechatronics Six d . o . f . displacement measuring device based on a modified Stewart platform, Mechatronics. 21 (2011) 1309–1316. doi:10.1016/j.mechatronics.2011.09.001.

[5] R. Wainscoat, The Pan-STARRS Search for Near Earth Objects, (2016).

[6] G.P. Lousberg, E. Mudry, C. Bastin, J. Schumacher, E. Gabriel, O. Pirnay, C. Flebus, A. Mechanical, O.S. Amos, C. Ardennais, Active optics system for the 4m telescope of the Eastern Anatolia Observatory (DAG), 9912 (2016) 1–9. doi:10.1117/12.2234261.

[7] Symétrie, SYMETRIE - Hexapode, Metrologie, Positionnement, Mesures, (2016). http://www.symetrie.fr/fr/ (accessed June 27, 2016).

[8] newport, Technical Note: Motion Basics and Standards, (2016).

[9] physik instrumente, PI Glossary for Technical Terms, (2016). http://www.physikinstrumente.com/info/glossary.html (accessed May 13, 2016).

[10] aerotech, Engineering Reference: Resolution , Accuracy and Repeatability, (2016) 1.

[11] B. Hromadka, T. Roux, M. Cuq, Metrology in high precision parallel positioning systems, in: Mechanical Engineering Design of Synchrotron Radiation Equipment and Instrumentation, shanghai, china, 2012.

[12] BIPM, International vocabulary of metrology - Basic and general concepts and associated terms (VIM), (2012).

[13] S.T. Smith, Foundations of ultraprecision mechanism design, CRC Press, 1992.

[14] A. Vissière, H. Nouira, M. Damak, O. Gibaru, J.-M. David, Concept and architecture of a new apparatus for cylindrical form measurement with a nanometric level of accuracy, Measurement Science and Technology. 23 (2012). doi:10.1088/0957-0233/23/9/094014.

[15] R. Leach, Fundamental Principles of Engineering Nanometrology, William Andrew, 2009.

[16] A.J. Fleming, Sensors and Actuators A: Physical A review of nanometer resolution position sensors: Operation and performance, Sensors & Actuators: A. Physical. 190 (2013) 106–126. doi:10.1016/j.sna.2012.10.016.

[17] A. Vissière, H. Nouira, M. Damak, O. Gibaru, Implementation of capacitive probes for ultra-high precision machine for cylindricity measurement with nanometre level of accuracy, International Journal of Precision Engineering and Manufacturing. 16 (2015) 883–893. doi:10.1007/s12541-015-0116-z.

[18] L. Precision, Understanding Sensor Resolution Specifications and Performance, 2009. http://www.lionprecision.com/tech-library/technotes/tech-pdfs/article-0010-sensor-resolution.pdf (accessed May 24, 2017).

[19] Fogale, Système de mesure capacitive MC900, (2012).

[20] BIPM, Evaluation of measurement data — Guide to the expression of uncertainty in measurement, 2008 (2008).

[21] BIPM, Evaluation of measurement data — Supplement 1 to the “Guide to the expression of uncertainty in measurement” — Propagation of

distributions using a Monte Carlo method, (2008).

[22] H. Schwenke, B.R.L. Siebert, F. Waldele, H. Kunzmann, Uncertainties in Dimensional Metrology by Monte Carlo Simulation: Proposal of a Modular and Visual Software, Annals of the CIRP. 49 (2000) 395–398.

[23] A. Klimchik, A. Pashkevich, S. Caro, D. Chablat, Stiffness matrix of manipulators with passive joints: computational aspects, (n.d.) 13–16.

[24] D. Daney, Etalonnage Geométrique des robots parallèles, Sophia Antipolis, 2000.

[25] H. Shi, H. Su, N. Dagalakis, J.A. Kramar, Kinematic modeling and calibration of a flexure based hexapod nanopositioner, Precision Engineering. 37 (2013) 117–128. doi:10.1016/j.precisioneng.2012.07.006.

[26] H. Nouira, A. Vissiere, M. Damak, J.-M. David, Investigation of the influence of the main error sources on the capacitive displacement measurements with cylindrical artefacts, Precision Engineering. 37 (2013) 721–737. doi:10.1016/j.precisioneng.2013.02.005.